

# A continuous time random walk model with multiple characteristic times

**Kwok Sau Fa and R S Mendes**

Departamento de Física, Universidade Estadual de Maringá, Avenida Colombo 5790, 87020-900, Maringá-PR, Brazil

E-mail: [kwok@dfi.uem.br](mailto:kwok@dfi.uem.br) and [rsmendes@dfi.uem.br](mailto:rsmendes@dfi.uem.br)

Received 8 January 2010

Accepted 27 February 2010

Published 1 April 2010

Online at [stacks.iop.org/JSTAT/2010/P04001](http://stacks.iop.org/JSTAT/2010/P04001)

[doi:10.1088/1742-5468/2010/04/P04001](https://doi.org/10.1088/1742-5468/2010/04/P04001)

**Abstract.** In this paper we consider a continuous time random walk (CTRW) model with a decoupled jump pdf. Further, we consider an approximate jump length pdf; for the waiting time pdf we do not use any approximation and we employ a function which depends on multiple characteristic times given by a sum of exponential functions. This waiting time pdf can reproduce power-law behavior for intermediate times. Using this specific waiting time probability density, we analyze the behavior of the second moment generated by the CTRW model. It is known that the waiting time pdf given by an exponential function generates a normal diffusion process, but for our waiting time pdf the second moment can give an anomalous diffusion process for intermediate times, and the normal diffusion process is maintained for the long-time limit. We note that systems which present subdiffusive behavior for intermediate times but reach normal diffusion at large times have been observed in biology.

**Keywords:** exact results, stochastic particle dynamics (theory), diffusion

---

**Contents**

<b>1. Introduction</b>	<b>2</b>
<b>2. The continuous time random walk model and the second moment for multiple characteristic times</b>	<b>4</b>
<b>3. The exact solution for the probability density</b>	<b>11</b>
<b>4. Conclusion</b>	<b>13</b>
<b>Acknowledgments</b>	<b>13</b>
<b>Appendix. The solution for <math>\rho(x, t)</math></b>	<b>14</b>
<b>References</b>	<b>15</b>

---

**1. Introduction**

Diffusion is a ubiquitous phenomenon, and it is one of the fundamental mechanisms for transport of materials in physical, chemical and biological systems. The most well-known example of a diffusion process is Brownian motion. Diffusion processes can be classified according to their mean square displacements

$$\langle x^2(t) \rangle \sim t^\alpha. \quad (1)$$

Anomalous diffusion has a mean square displacement that deviates from linear time dependence. The process is called subdiffusive when  $0 < \alpha < 1$  and superdiffusive when  $\alpha > 1$ . Nowadays, there are several approaches for describing anomalous diffusion processes, and they can be applied to many situations of natural systems [1]–[9]. One of the most interesting features incorporated into these approaches is the memory effect. In particular, the memory effect incorporated into the Langevin approach, referred to as the generalized Langevin equation (GLE) [4], can be associated with the retardation of friction and fractal media [10, 11]. Moreover, according to the fluctuation-dissipation theorem [1], the internal friction is directly related to the correlation function of the random force.

In many situations, a finite correlated noise is necessary for describing the real systems in equilibrium states. However, in order to describe anomalous diffusion, a nonlocal friction should be employed, satisfying the fluctuation-dissipation theorem. For instance, anomalous diffusion processes have been observed in a variety of systems such as bacterial cytoplasm motion [12], conformational fluctuations within a single protein molecule [13] and fluorescence intermittency in single enzymes [14]. These processes have been described using the GLE, and a memory effect has also been shown using generalized Fokker–Planck equations (GFPE) [4]. It should be noted that other models may also be considered for describing these systems.

In particular, the continuous time random walk (CTRW) [15] can also be employed to describe anomalous diffusion [16]–[22]. Further, the CTRW with a power-law waiting time probability density function (pdf) [23, 24] was linked to the following fractional Fokker–

Planck equation [5]:

$$\frac{\partial \rho(x, t)}{\partial t} = {}_0D_t^{1-\alpha} K_\alpha \frac{\partial^2}{\partial x^2} \rho(x, t), \quad (2)$$

where

$${}_0D_t^{1-\alpha} \rho(x, t) = \frac{1}{\Gamma(\alpha)} \frac{\partial}{\partial t} \int_0^t \frac{\rho(x, t_1)}{(t - t_1)^{1-\alpha}} dt_1 \quad (3)$$

is the Riemann–Liouville fractional derivative and  $\Gamma(z)$  is the Gamma function.  $\rho(x, t) dx$  is the probability for finding a particle in a position between  $x$  and  $x + dx$  at time  $t$ . It should be noted that the memory effect in the GLE approach appears on the level of the stochastic equation but leads to time-dependent coefficients on the noise-averaged level. In contrast to the GLE approach, the subdiffusive CTRW model has a memory kernel on the noise-averaged level.

The CTRW model may be described using a set of Langevin equations [5, 25, 26] or an appropriate generalized master equation [19, 27, 28]. The pdf  $\rho(x, t)$  obeys the following equation in Fourier–Laplace space [5]:

$$\rho(k, s) = \frac{1 - g(s)}{s} \frac{\rho_0(k)}{1 - \psi(k, s)}, \quad (4)$$

where  $\rho_0(k)$  is the Fourier transform of the initial condition  $\rho_0(x)$ ,  $\psi(x, t)$  is the jump pdf and  $g(t)$  is the waiting time pdf defined by

$$g(t) = \int_{-\infty}^{\infty} \psi(x, t) dx. \quad (5)$$

Moreover, from the jump pdf we also have the jump length pdf defined by

$$\phi(x) = \int_0^{\infty} \psi(x, t) dt. \quad (6)$$

In many cases, the CTRW model can be simplified through the decoupled jump pdf  $\psi(k, s) = \phi(k)g(s)$ . In particular, we consider a finite jump length variance. In this case we can take, for instance, a Gaussian jump length pdf, and its lowest order in Fourier space is given by [5]

$$\phi(k) \sim 1 - Dk^2 + O(k^4). \quad (7)$$

In fact, any jump length pdf with finite variance leads to this small  $k$  behavior, and in the continuum limit only the lowest order enters into the CTRW theory. In this situation, different kinds of CTRW models are specified through specifying the waiting time pdf. The CTRW model is also connected to a class of Fokker–Planck equations [5, 29]. Furthermore, in the CTRW model, solutions for  $\rho(x, t)$  under the condition of a long-tailed waiting time pdf can be found in [30]–[32].

Substituting equation (7) into (4), we have

$$\rho(k, s) = \frac{1 - g(s)}{s} \frac{\rho_0(k)}{1 - (1 - Dk^2)g(s)}. \quad (8)$$

It should be noted that the CTRW model can be classified according to the characteristic waiting time  $T$  and the jump length variance  $\Sigma^2$  defined by

$$T = \int_0^{\infty} t g(t) dt, \quad (9)$$

and

$$\Sigma^2 = \int_{-\infty}^{\infty} x^2 \phi(x) dx. \quad (10)$$

For finite  $T$  and  $\Sigma^2$ , the long-time limit corresponds to Brownian motion [5]. Although equation (8) is valid for a finite jump length variance, anomalous diffusion can be produced by equation (8) with appropriate choices of waiting time pdf. With this perspective, we propose to investigate some interesting aspects of anomalous diffusion processes related to the CTRW model. Moreover, anomalous diffusion is a subject of great current interest.

The aim of this work is to investigate the behavior of a particle's diffusion with a specified waiting time pdf given by a sum of  $N$  exponential functions. We should note an interesting aspect of this waiting time pdf; it can describe power-law behavior for intermediate times and exponential behavior for the long-time limit. Moreover, the greater the value of  $N$ , the greater the range for the power-law behavior. For this case the particle spends more time in a specified site for intermediate times, and it can describe anomalous behaviors. However, in the long-time limit the system recovers the usual diffusive process due to the exponential behavior of the waiting time pdf which gives a finite characteristic waiting time. We note that this kind of regime has been observed in biological systems [33]–[35]. This paper is organized as follows. In section 2 we study the CTRW model through the second moment using a waiting time pdf with multiple characteristic times. In section 3, we show the exact solutions for the pdf  $\rho(x, t)$ . Finally, conclusions are presented in section 4.

## 2. The continuous time random walk model and the second moment for multiple characteristic times

Equation (8) was already employed for studying diffusion behavior when the form of the waiting time pdf  $g(t)$  was first specified, e.g., as a power-law function in the long-time limit [5]. In this case, the corresponding fractional differential equation is given by equation (2). For  $\alpha = 1$ , equation (2) gives the well-known ordinary diffusion equation. For a generic form of  $g(t)$  the corresponding integro-differential equation for CTRW can be described via the following equation [36]:

$$\frac{\partial \rho(x, t)}{\partial t} - \int_0^t g(t - t_1) \frac{\partial \rho(x, t_1)}{\partial t_1} dt_1 = D \frac{\partial}{\partial t} \int_0^t g(t - t_1) \frac{\partial^2 \rho(x, t_1)}{\partial x^2} dt_1. \quad (11)$$

We note that equation (11) has a different form to the ones described in [27, 37]. In order to obtain equation (11) we first apply the inverse Fourier transform to equation (8) and we obtain

$$\rho(x, s) - \frac{1}{s} \rho(x, 0) - g(s) \rho(x, s) + \frac{1}{s} g(s) \rho(x, 0) = D g(s) \frac{\partial^2 \rho(x, s)}{\partial x^2}. \quad (12)$$

Now we apply the inverse Laplace transform to equation (12); we have

$$\begin{aligned} \rho(x, t) - \rho(x, 0) - \int_0^t g(t - t_1) \rho(x, t_1) dt_1 + \rho(x, 0) \int_0^t g(t_1) dt_1 \\ = D \int_0^t g(t - t_1) \frac{\partial^2 \rho(x, t_1)}{\partial x^2} dt_1. \end{aligned} \quad (13)$$

Applying the operator  $\partial/\partial t$  to equation (13), one can obtain the integro-differential equation (11).

For the case of  $g(t) = t^{\alpha-1}/\Gamma(\alpha)$ , the integrals of equation (11) become the Caputo or the Riemann–Liouville fractional derivatives. The difference between them is that the Caputo fractional derivative requires the integrability of the derivative and contains the initial value of the function. Therefore the Caputo fractional derivative is more restrictive than the Riemann–Liouville fractional derivative. However, if the initial values are properly taken into account, the two formulations are equivalent. It should be pointed out that the use of these operators may lead to different behaviors including unphysical behavior in different systems [38, 39]. Equation (11) is derived from a well-defined physical process, and no ambiguities and unphysical behaviors are expected. The left side of equation (11) shows the variation of  $\rho(x, t)$  with respect to time, which depends not only on the ordinary derivative operator but also on the difference between ordinary and nonlocal integral operators.

Equation (11) can be used for obtaining the second moment. We note that

$$\frac{d\langle x^2 \rangle}{dt} = \int_{-\infty}^{\infty} x^2 \frac{\partial \rho(x, t)}{\partial t} dx. \quad (14)$$

Substituting equation (11) into (14) yields

$$\frac{d\langle x^2 \rangle}{dt} = \int_0^t g(t - t_1) \frac{d\langle x^2 \rangle}{dt_1} dt_1 + D \frac{\partial}{\partial t} \int_0^t g(t - t_1) \int_{-\infty}^{\infty} x^2 \frac{\partial^2 \rho(x, t)}{\partial x^2} dx dt_1. \quad (15)$$

After integrating the second term of the right side of equation (15) by parts twice, we have

$$\frac{d\langle x^2 \rangle}{dt} = \int_0^t g(t - t_1) \frac{d\langle x^2 \rangle}{dt_1} dt_1 + 2D \frac{\partial}{\partial t} \int_0^t g(t - t_1) \int_{-\infty}^{\infty} \rho(x, t) dx dt_1, \quad (16)$$

where we also consider that  $\lim_{x \rightarrow \pm\infty} \rho(x, t)$  and it decreases faster than  $1/x$ . The normalization of the pdf  $\rho(x, t)$  requires that  $\int_{-\infty}^{\infty} \rho(x, t) dx = 1$ . Finally, equation (16) can be rewritten as

$$\frac{d\langle x^2 \rangle}{dt} = \int_0^t g(t - t_1) \frac{d\langle x^2 \rangle}{dt_1} dt_1 + 2D \frac{\partial}{\partial t} \int_0^t g(t - t_1) dt_1. \quad (17)$$

Employing the Laplace transform in equation (17) we obtain

$$\langle x^2 \rangle_L = \frac{\langle x^2 \rangle_0}{s} + \frac{2Dg(s)}{s[1 - g(s)]} \quad (18)$$

in Laplace space. We have shown that for equation (11), even for a generic waiting time pdf, the second moment of displacement can be directly obtained from equation (18).

Thus, different diffusion behaviors can be found when substituting different waiting time pdfs into equation (18).

Considering that the waiting time pdf must be positive and normalizable; there exist only a few simple functions that can be used as waiting time pdfs. Now we propose a more complicated form of waiting time pdf and investigate diffusion behaviors generated with it. Our proposal is made up of a sum of exponential functions, which is given by

$$g(t) = A_N \sum_{i=0}^N c_i e^{-\lambda_i t}, \quad (19)$$

where  $c_i$  and  $\lambda_i$  are constants, and  $A_N$  is a normalization constant given by

$$A_N = \frac{1}{\sum_{i=0}^N c_i / \lambda_i}. \quad (20)$$

We also consider  $\lambda_i > 0$ . A multiexponential model can be found for excited-state decay systems, for instance for a system of emitting residues, with the assumption of noninteracting resonance transitions [40]. Moreover, many positive functions can be well approximated by a finite sum of exponential function indicating that the waiting time pdf can contain several characteristic times. In particular, we should note an interesting aspect of the waiting time pdf (19); for an appropriate choice of  $c_i$  and  $\lambda_i$  the function  $g(t)$  can describe power-law behavior with logarithmic oscillations for intermediate times and exponential behavior for the long-time limit. Moreover, the greater the value of  $N$ , the greater the range for the power-law behavior. In contrast to the pure power-law function, which is not normalizable, the waiting time pdf (19) is normalizable and its characteristic waiting time is also finite,  $T = A_N \sum_{i=0}^N c_i / \lambda_i^2$ , for  $N$  finite; then, the long-time limit corresponds to the normal diffusion.

The Laplace transform of  $g(t)$  is given by

$$g(s) = A_N \sum_{i=0}^N \frac{c_i}{\lambda_i + s}. \quad (21)$$

Substituting equation (21) into (18) we have

$$\frac{\langle x^2 \rangle_L}{2D} = -\frac{1}{s} + \frac{1}{s^2} \frac{PN_{N+1} + PN_N s + PN_{N-1} s^2 + \dots + PN_1 s^N + PN_0 s^{N+1}}{KN_N + KN_{N-1} s + KN_{N-2} s^2 + \dots + KN_1 s^{N-1} + s^N}, \quad (22)$$

where the coefficients  $PN_i$  and  $KN_i$  correspond to the expansions of  $(\lambda_0 + s) \dots (\lambda_N + s)$  and  $(\lambda_0 + s) \dots (\lambda_N + s) - A_N [c_0(\lambda_1 + s) \dots (\lambda_N + s) + c_1(\lambda_0 + s)(\lambda_2 + s) \dots (\lambda_N + s) + c_2(\lambda_0 + s)(\lambda_1 + s)(\lambda_3 + s) \dots (\lambda_N + s) + c_N(\lambda_0 + s) \dots (\lambda_{N-1} + s)]$ , respectively. The second moment is given by

$$\begin{aligned} \frac{\langle x^2 \rangle}{2D} = & -1 + \sum_{m_N=0}^{\infty} \frac{[-KN_N t^N]^{m_N}}{m_N!} \sum_{m_{N-1}=0}^{\infty} \frac{[-KN_{N-1} t^{N-1}]^{m_{N-1}}}{m_{N-1}!} \dots \sum_{m_1=0}^{\infty} \frac{[-KN_1 t]^{m_1}}{m_1!} \\ & \times \left( \sum_{i=1}^N m_{i1} \right)! \left[ \sum_{j=0}^{N+1} \frac{PN_j t^j}{\Gamma \left( \sum_{i=2=1}^N (i2) m_{i2} + j + 1 \right)} \right], \quad (23) \end{aligned}$$

for  $N \geq 1$ . We note that one can write equation (23) in terms of the generalized Mittag-Leffler function as follows. First, we rewrite equation (23) as

$$\frac{\langle x^2 \rangle}{2D} = -1 + \sum_{m_N=0}^{\infty} \frac{[-KN_N t^N]^{m_N}}{m_N!} \dots \sum_{m_2=0}^{\infty} \frac{[-KN_2 t^2]^{m_2}}{m_2!} \times \left[ \sum_{j=0}^{N+1} \left( PN_j t^j \sum_{m_1=0}^{\infty} \frac{\left(\sum_{i_1=1}^N m_{i_1}\right)! [-KN_1 t]^{m_1}}{m_1! \Gamma\left(\sum_{i_2=1}^N (i_2) m_{i_2} + j + 1\right)} \right) \right]. \quad (24)$$

The summation inside the parenthesis can be written in terms of the generalized Mittag-Leffler function

$$\frac{\langle x^2 \rangle}{2D} = -1 + \sum_{m_N=0}^{\infty} \frac{[-KN_N t^N]^{m_N}}{m_N!} \dots \sum_{m_2=0}^{\infty} \frac{[-KN_2 t^2]^{m_2}}{m_2!} \times \left[ \sum_{j=0}^{N+1} PN_j t^j E_{1, j+1+\sum_{i_2=1}^{N-1} (i_2) m_{i_2+1}}^{(\sum_{i_1=1}^{N-1} m_{i_1+1})} (-KN_1 t) \right], \quad (25)$$

where  $E_{\mu, \nu}(y)$  is defined by [41, 42]

$$E_{\mu, \nu}(y) = \sum_{m=0}^{\infty} \frac{y^m}{\Gamma(\nu + \mu m)} \quad (26)$$

and

$$E_{\mu, \nu}^n(y) = \frac{d^n}{dy^n} E_{\mu, \nu}(y) = \sum_{m=0}^{\infty} \frac{(m+n)! y^m}{\Gamma(\nu + \mu(m+n))}. \quad (27)$$

Equation (25) has the following asymptotic behavior ( $t \gg 1$ ):

$$\frac{\langle x^2 \rangle}{2D} \sim -1 + \frac{PN_N}{KN_N} - \frac{PN_{N+1}KN_{N-1}}{(KN_N)^2} + \frac{PN_{N+1}}{KN_N} t, \quad (28)$$

and it describes normal diffusive behavior.

In order to show some interesting aspects of the CTRW model with the waiting time pdf (19) we consider specific choices of  $c_i$  and  $\lambda_i$ . For the first case, we consider  $N = 1$ ,  $\lambda_0 = b_1$ ,  $\lambda_1 = b_2$  and  $A_1 = 1$ . In particular, this model can reproduce the mean square displacement of the Langevin equation for Brownian motion of a particle with an inertial term. The normalization of  $g(t)$  implies that

$$c_0 = b_1 \left( 1 - \frac{c_1}{b_2} \right). \quad (29)$$

Substituting equation (29) into (18) we obtain

$$\langle (x - x_0)^2 \rangle = \frac{2d}{E_3^2} [-(E_2 - E_1 E_3)(1 - e^{-E_3 t}) + E_2 E_3 t], \quad (30)$$

where

$$E_1 = b_1 + \left(1 - \frac{b_1}{b_2}\right) c_1, \quad (31)$$

$$E_2 = b_1 b_2 \quad (32)$$

and

$$E_3 = b_2 - \left(1 - \frac{b_1}{b_2}\right) c_1. \quad (33)$$

Now we can compare the result (30) with that of the Langevin equation for Brownian motion [3]. This system is described by the following equation:

$$\frac{dv(t)}{dt} + \gamma v(t) = \Theta(t), \quad (34)$$

where  $\Theta(t)$  is the Langevin force with zero mean,  $\langle \Theta(t) \rangle = 0$ , and the correlation function given by  $\langle \Theta(t_1) \Theta(t_2) \rangle = q \delta(t_1 - t_2)$ , and  $\delta(t)$  is the Dirac delta function. The mean square displacement of the Brownian motion of a particle is given by

$$\langle (x - x_0)^2 \rangle = \left(v_0^2 - \frac{q}{2\gamma}\right) \frac{(1 - e^{-\gamma t})^2}{\gamma^2} - \frac{q}{\gamma^3} (1 - e^{-\gamma t}) + \frac{q}{\gamma^2} t \quad (35)$$

and the diffusion constant  $K$  given by  $K = q/(2\gamma^2)$ .

In order to reproduce the result (35) from equation (30) we first consider the initial velocity distribution for the stationary state given by  $\langle v_0^2 \rangle = q/(2\gamma)$ . Then, from equation (35) we have

$$\langle (x - x_0)^2 \rangle = -\frac{q}{\gamma^3} (1 - e^{-\gamma t}) + \frac{q}{\gamma^2} t, \quad (36)$$

and from equations (30) to (33) we have

$$b_1 = \frac{q}{D\gamma^2} \frac{1}{(1 \pm \sqrt{1 - (2q/D\gamma^3)})}, \quad b_2 = \frac{\gamma}{2} \left(1 \pm \sqrt{1 - \frac{2q}{D\gamma^3}}\right), \quad c_0 = -c_1, \quad (37)$$

$$E_1 = 0, \quad E_2 = \frac{q}{2D\gamma} \quad \text{and} \quad E_3 = \gamma. \quad (38)$$

These results give the Langevin approach and CTRW model as closely related to each other. In fact, in the Langevin equation (34) the parameters  $\gamma$  and  $q$  are related to the macroscopic and microscopic characteristic times, respectively. In the CTRW model these quantities are related to the parameters  $b_1$  and  $b_2$  of the waiting time pdf. Notice that the mean square displacement (36) has ballistic diffusion for short time and eventually reaches normal diffusion.



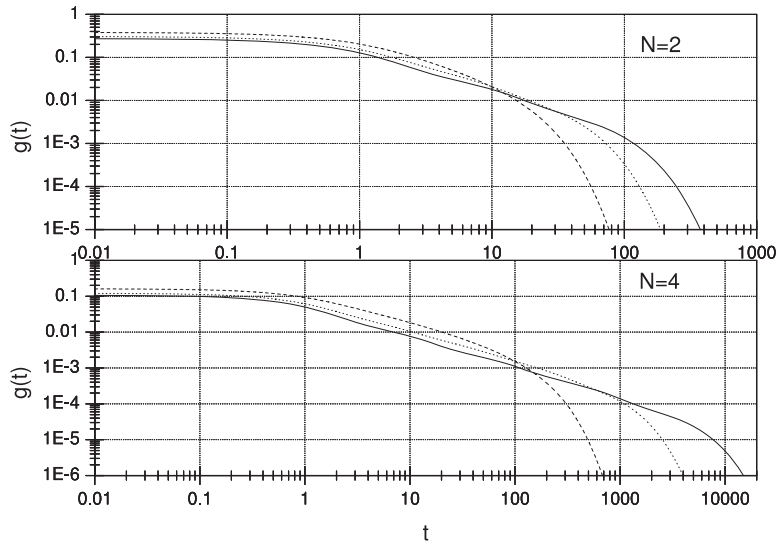


**Figure 1.** Plots of  $g(t)$  for different values of  $a$  and  $b$ . The solid lines correspond to  $a = 2/15$  and  $b = 0.7$ . The dotted lines correspond to  $a = 3/15$  and  $b = 0.7$ , and the dashed lines correspond to  $a = 5/15$  and  $b = 0.7$ .

For the second case, we take  $c_i = (a/b)^i > 0$  and  $\lambda_i = a^i$ , and we obtain

$$A_N = \frac{1}{\sum_{m=0}^N 1/b^m}. \quad (39)$$

In figure 1 we show  $g(t)$  for  $N = 2$  and 4. We note that  $g(t)$  can approximately describe power-law behavior for intermediate times and it decays exponentially in the long-time limit. Moreover, the greater the value of  $N$ , the greater the range for the power-law behavior. We also note that in addition to this power-law main trend, there occur subdominant logarithmic oscillations [43, 44] (as can be identified in figure 1). If  $g(t)$  is not a discrete sum of exponentials but a sum in the continuum limit (given by an integral), then logarithmic oscillations could not occur [45]. This kind of self-similar structure ( $N \rightarrow \infty$ ) was initially considered in the economic context [46] and subsequently in other systems such as physical, chemical and biological systems (see [43]–[45], [47] and references therein). These facts reinforce our belief that the diffusive process based on the above waiting time pdf may be useful in the discussion of systems with many timescales.

Now we consider  $N = 2$ . From equation (23) we obtain

$$\begin{aligned} \frac{\langle x^2 \rangle}{2D} = & -1 + \sum_{m_2=0}^{\infty} \frac{[-K2_2 t^2]^{m_2}}{m_2!} \sum_{m_1=0}^{\infty} \frac{[-K2_1 t]^{m_1} (m_1 + m_2)!}{m_1!} \left[ \frac{a^3 t^3}{\Gamma(2m_2 + m_1 + 4)} \right. \\ & \left. + \frac{a(1 + a + a^2)t^2}{\Gamma(2m_2 + m_1 + 3)} + \frac{(1 + a + a^2)t}{\Gamma(2m_2 + m_1 + 2)} + \frac{1}{\Gamma(2m_2 + m_1 + 1)} \right], \end{aligned} \quad (40)$$

where the term  $\langle x^2 \rangle_0/s$  has been omitted, and

$$K2_1 = 1 + a + a^2 - A_2 \left( 1 + \frac{a}{b} + \left( \frac{a}{b} \right)^2 \right) \quad (41)$$

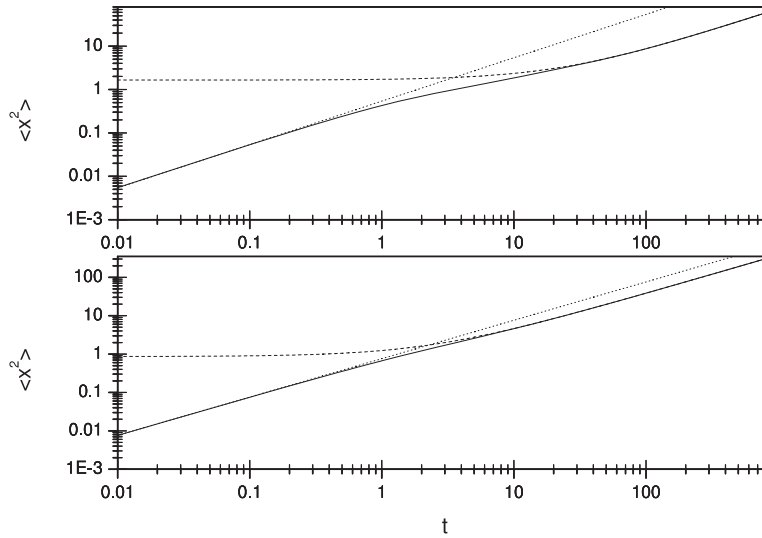


**Figure 2.** Plots of  $\langle x^2 \rangle$  for different values of  $a$  and  $b$  with  $N = 2$ . The upper and lower figures correspond to  $a = 2/15, 5/15$  and  $b = 0.7$ , respectively. The solid lines are obtained from equation (40) and the dashed lines are the asymptotic curves obtained from equation (43). The dotted lines correspond to linear functions given by  $0.54t$  (for the upper figure) and  $0.75t$  (for the lower figure).

and

$$K2_2 = a(1 + a + a^2) - A_2 \left( a + a^2 + \frac{a}{b}(1 + a^2) + \left(\frac{a}{b}\right)^2 (1 + a) \right). \quad (42)$$

The asymptotic limit of equation (40) is given by

$$\frac{\langle x^2 \rangle}{2D} \sim -1 - \frac{a^3 K2_1}{(K2_2)^2} + \frac{a(1 + a + a^2)}{K2_2} + \frac{a^3}{K2_2} t. \quad (43)$$

In figure 2 we show the behavior of  $\langle x^2 \rangle$  for different values of  $a$  and  $b$ . It deviates from the normal diffusion for intermediate times and the normal diffusion behavior is maintained in the long-time limit. We see that the beginning and the end of the subdiffusive behavior coincide with the power-law behavior of figure 1.

For  $N = 4$  we have

$$\begin{aligned} \frac{\langle x^2 \rangle}{2D} = & -1 + \sum_{m_4=0}^{\infty} \frac{[-K4_4 t^4]^{m_4}}{m_4!} \sum_{m_3=0}^{\infty} \frac{[-K4_3 t^3]^{m_3}}{m_3!} \sum_{m_2=0}^{\infty} \frac{[-K4_2 t^2]^{m_2}}{m_2!} \\ & \times \sum_{m_1=0}^{\infty} \frac{[-K4_1 t]^{m_1} (m_1 + m_2 + m_3 + m_4)!}{m_1!} \left[ \frac{a^{10} t^5}{\Gamma(4m_4 + 3m_3 + 2m_2 + m_1 + 6)} \right. \\ & \left. + \frac{P4_4 t^4}{\Gamma(4m_4 + 3m_3 + 2m_2 + m_1 + 5)} + \frac{P4_3 t^3}{\Gamma(4m_4 + 3m_3 + 2m_2 + m_1 + 4)} \right] \end{aligned}$$

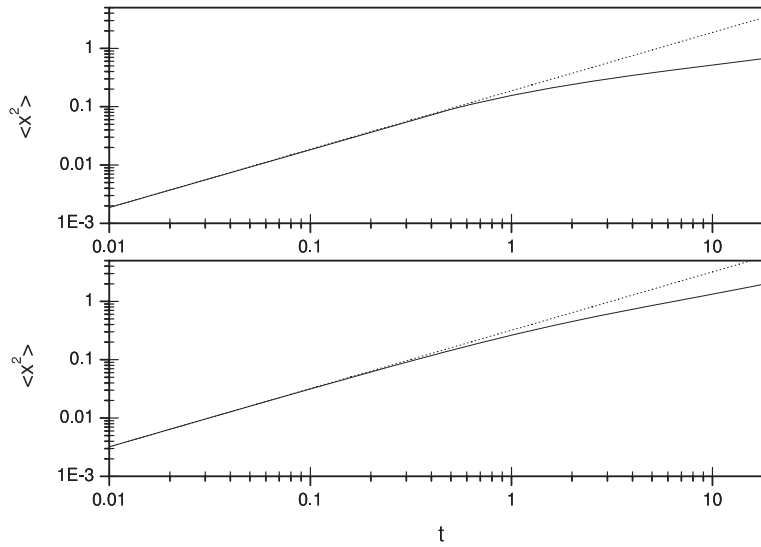


**Figure 3.** Plots of  $\langle x^2 \rangle$  for different values of  $a$  and  $b$  with  $N = 4$ . The upper and lower figures correspond to  $a = 2/15, 5/15$  and  $b = 0.7$ , respectively. The solid lines are obtained from equation (44). The dotted lines correspond to linear functions given by  $0.187t$  (for the upper figure) and  $0.32t$  (for the lower figure).

$$\begin{aligned}
 & + \frac{P4_2 t^2}{\Gamma(4m_4 + 3m_3 + 2m_2 + m_1 + 3)} + \frac{P4_1 t}{\Gamma(4m_4 + 3m_3 + 2m_2 + m_1 + 2)} \\
 & + \frac{1}{\Gamma(4m_4 + 3m_3 + 2m_2 + m_1 + 1)} \Big]. \tag{44}
 \end{aligned}$$

The asymptotic limit of equation (44) is given by

$$\frac{\langle x^2 \rangle}{2D} \sim -1 + \frac{P4_4}{K4_4} - \frac{a^{10} K4_3}{(K4_4)^2} + \frac{a^{10}}{K4_4} t. \tag{45}$$

In figure 3 we show the behavior of  $\langle x^2 \rangle$  for different values of  $a$  and  $b$ . We see that the behavior of  $\langle x^2 \rangle$  deviates from the normal diffusion for intermediate times. The normal diffusion behavior is maintained in the long-time limit (45).

### 3. The exact solution for the probability density

Generally speaking, using equation (4) one can calculate the pdf in the framework of the CTRW model. However, it is hard to obtain the exact pdf from equation (4). In particular, we can obtain the exact solution for  $\rho(x, t)$  in the case of the waiting time pdf given in section 2. In the following, we consider the initial condition as  $\rho_0(k) = 1$ . After we take the Fourier inverse for  $\rho(k, s)$  in equation (8), we have

$$\rho(x, s) = \frac{1 - g(s)}{2\pi D s g(s)} \int_{-\infty}^{\infty} \frac{e^{ikx}}{k^2 + ((1 - g(s))/Dg(s))} dk. \tag{46}$$

We note that the denominator can have three different poles:  $1 - g(s) = 0$  gives the trivial result,  $(1 - g(s))/g(s) < 0$  gives the poles on the real axis and  $(1 - g(s))/g(s) > 0$  gives the

poles on the imaginary axis. For the waiting time pdf given in section 2 we can restrict to the case of the poles on the imaginary axis. Thus, the solution for  $\rho(x, s)$  is given by

$$\rho(x, s) = \frac{1}{2\sqrt{Ds}} \sqrt{\frac{1-g(s)}{g(s)}} \exp\left(-\frac{|x|}{\sqrt{D}} \sqrt{\frac{1-g(s)}{g(s)}}\right). \quad (47)$$

Before obtaining the exact solutions to  $\rho(x, t)$  we can calculate the second moment in Laplace space which yields

$$\langle x^2 \rangle_L = \frac{2Dg(s)}{s[1-g(s)]}. \quad (48)$$

This result is similar to (18), except for the term of the initial value  $\langle x^2 \rangle_0$ .

For the waiting time pdf (19) the solution for  $\rho_N(x, t)$  can be obtained from equation (47) and it is given in the appendix.

The asymptotic expansion of  $\rho_N(x, t)$  (for finite  $x$  and  $t \gg 1$ ) is given by

$$\rho_N(x, t) \sim \frac{1}{2} \sqrt{\frac{KN_N}{\pi D \left(\prod_{l=0}^N \lambda_l\right) t}}. \quad (49)$$

It is worth mentioning that the pdf  $\rho_N(x, t)$  shows the same power-law decay  $1/\sqrt{t}$  of the normal diffusion for all  $N$ , and it is also independent of the spatial coordinate  $x$ . This result is not a surprise because the waiting time pdf (19) has a finite characteristic waiting time.

As examples, we now present the solutions for the cases discussed in the previous section with  $N = 1$  and 2. For the case of  $N = 1$  (see equation (29)) the solution for  $\rho(x, t)$  is given by

$$\begin{aligned} \rho_1(x, t) = & \frac{1}{\pi} \int_0^\infty d\omega \Phi_1(\omega) \cos\left(\omega t - \frac{\pi}{2} + \frac{1}{2} \arccos\left(-\frac{\omega^2}{r'_1}\right)\right) \\ & - \frac{|x|\sqrt{r'_1}}{\sqrt{Db_1b_2}} \sin\left(\frac{1}{2} \arccos\left(-\frac{\omega^2}{r'_1}\right)\right) d\omega, \end{aligned} \quad (50)$$

where

$$r'_1 = [\omega^4 + \omega^2(b_1 + b_2)^2]^{1/2} \quad (51)$$

and

$$\Phi_1(\omega) = \frac{\sqrt{r'_1}}{2\sqrt{Db_1b_2}\omega} \exp\left(-\frac{|x|\sqrt{r'_1}}{\sqrt{Db_1b_2}} \cos\left(\frac{1}{2} \arccos\left(-\frac{\omega^2}{r'_1}\right)\right)\right). \quad (52)$$

For  $N = 2$  the solution for  $\rho(x, t)$  is given by

$$\begin{aligned} \rho_2(x, t) = & \frac{1}{\pi} \int_0^\infty d\omega \Phi_2(\omega) \cos\left(\omega t - \frac{\pi}{2} + \frac{1}{2} \arccos\left(\frac{A_{22}}{r_2}\right)\right) \\ & - \frac{|x|\sqrt{r_2}}{\sqrt{DA_{23}}} \sin\left(\frac{1}{2} \arccos\left(\frac{A_{22}}{r_2}\right)\right) d\omega, \end{aligned} \quad (53)$$

where

$$r_2 = [A_{21}^2 + A_{22}^2]^{1/2}, \quad (54)$$

$$A_{21} = \{\lambda_0\lambda_1 + \lambda_0\lambda_2 + \lambda_1\lambda_2 - A_2[c_0(\lambda_1 + \lambda_2) + c_1(\lambda_0 + \lambda_2) + c_2(\lambda_0 + \lambda_1)] - \omega^2\} \\ \times [\lambda_0\lambda_1\lambda_2 + A_2(c_0 + c_1 + c_2)\omega^2]\omega + A_2[c_0(\lambda_1 + \lambda_2) + c_1(\lambda_0 + \lambda_2) \\ + c_2(\lambda_0 + \lambda_1)][\lambda_0 + \lambda_1 + \lambda_2 - A_2(c_0 + c_1 + c_2)]\omega^3, \quad (55)$$

$$A_{22} = \{\lambda_0\lambda_1 + \lambda_0\lambda_2 + \lambda_1\lambda_2 - A_2[c_0(\lambda_1 + \lambda_2) + c_1(\lambda_0 + \lambda_2) + c_2(\lambda_0 + \lambda_1)] - \omega^2\} \\ \times [c_0(\lambda_1 + \lambda_2) + c_1(\lambda_0 + \lambda_2) + c_2(\lambda_0 + \lambda_1)]A_2\omega^2 \\ - [\lambda_0 + \lambda_1 + \lambda_2 - A_2(c_0 + c_1 + c_2)][\lambda_0\lambda_1\lambda_2 + A_2(c_0 + c_1 + c_2)\omega^2]\omega^2, \quad (56)$$

$$A_{23} = \{[\lambda_0\lambda_1\lambda_2 + A_2(c_0 + c_1 + c_2)\omega^2]^2 + [c_0(\lambda_1 + \lambda_2) + c_1(\lambda_0 + \lambda_2) + c_2(\lambda_0 + \lambda_1)]^2 \\ \times A_2^2\omega^2\}^{1/2} \quad (57)$$

and

$$\Phi_2(\omega) = \frac{\sqrt{r_2}}{2\sqrt{D}A_{23}\omega} \exp\left(-\frac{|x|\sqrt{r_2}}{\sqrt{D}A_{23}} \cos\left(\frac{1}{2} \arccos\left(\frac{A_{22}}{r_2}\right)\right)\right). \quad (58)$$

#### 4. Conclusion

In this work we have proposed and investigated the waiting time pdf described as a sum of exponential functions (19) in the framework of the CTRW model with a decoupled jump pdf. This kind of waiting time pdf can be used to describe power-law behavior for intermediate times; the greater the value of  $N$ , the greater the range for the power-law behavior (figure 1). This suggests that the waiting time pdf (19) may be used as an alternative for describing power-law behavior, using multiple characteristic times. As a consequence, subdiffusive behavior can be generated at the intermediate times; figures 2 and 3 show this behavior clearly. Moreover, we have presented exact solutions for the second moment and the probability density for a generic  $N$ . In particular, we have shown a very interesting result for  $N = 1$  which can reproduce the mean square displacement of the Langevin equation for Brownian motion of a particle with an inertial term. The two characteristic times present in the Langevin approach have counterparts in the framework of the CTRW given by the parameters  $b_1$  and  $b_2$ ; this result shows that the multiexponential waiting time pdf may be a useful tool for describing physical systems.

Finally, we hope that the waiting time pdf (19) may also be useful for describing chemical and biological systems.

#### Acknowledgments

KSF and RSM acknowledge partial financial support from the Conselho Nacional de Desenvolvimento Científico e Tecnológico (CNPq), Brazilian agency.

**Appendix. The solution for  $\rho(x, t)$**

For the waiting time pdf (19) the solution for  $\rho(x, t)$  can be described as follows. In the case of  $N$  being an even number, the solution is given by

$$\rho_N(x, t) = \frac{1}{\pi} \int_0^\infty d\omega \Phi_N(\omega) \cos\left(\omega t - \frac{\pi}{2} + \frac{1}{2} \arccos\left(\frac{A_{N2}}{r_N}\right) - \frac{|x|\sqrt{r_N}}{\sqrt{D}A_{N3}} \sin\left(\frac{1}{2} \arccos\left(\frac{A_{N2}}{r_N}\right)\right)\right) d\omega, \quad (\text{A.1})$$

where

$$A_{N1} = \sum_{j=0}^{N/2} (-1)^j K N_{N-2j} \omega^{1+2j} \left[ \sum_{l=0}^{N/2-1} (-1)^{1+l} (P N_{N-1-2l} - K N_{N-1-2l}) \omega^{2(1+l)} + \prod_{l=0}^N \lambda_l \right] - \sum_{j=0}^{N/2-1} (-1)^{1+j} K N_{N-1-2j} \omega^{2(1+j)} \left[ \sum_{l=0}^{N/2-1} (-1)^l (P N_{N-2l} - K N_{N-2l}) \omega^{1+2l} \right], \quad (\text{A.2})$$

$$A_{N2} = \sum_{j=0}^{N/2-1} (-1)^{1+j} K N_{N-1-2j} \omega^{2(1+j)} \times \left[ \sum_{l=0}^{N/2-1} (-1)^{1+l} (P N_{N-1-2l} - K N_{N-1-2l}) \omega^{2(1+l)} + \prod_{l=0}^N \lambda_l \right] + \sum_{j=0}^{N/2} (-1)^j K N_{N-2j} \omega^{1+2j} \left[ \sum_{l=0}^{N/2-1} (-1)^l (P N_{N-2l} - K N_{N-2l}) \omega^{1+2l} \right], \quad (\text{A.3})$$

$$A_{N3} = \left\{ \left[ \prod_{l=0}^N \lambda_l + \sum_{l=0}^{N/2-1} (-1)^{1+l} (P N_{N-1-2l} - K N_{N-1-2l}) \omega^{2(1+l)} \right]^2 + \left[ \sum_{l=0}^{N/2-1} (-1)^l (P N_{N-2l} - K N_{N-2l}) \omega^{1+2l} \right]^2 \right\}^{1/2}, \quad (\text{A.4})$$

$$\Phi_N(\omega) = \frac{\sqrt{r_N}}{2\sqrt{D}A_{N3}\omega} \exp\left(-\frac{|x|\sqrt{r_N}}{\sqrt{D}A_{N3}} \cos\left(\frac{1}{2} \arccos\left(\frac{A_{N2}}{r_N}\right)\right)\right) \quad (\text{A.5})$$

and

$$r_N = \sqrt{A_{N1}^2 + A_{N2}^2}. \quad (\text{A.6})$$

In the case of  $N$  being an odd number, the solution is given by

$$\rho_N(x, t) = \frac{1}{\pi} \int_0^\infty d\omega \Phi_N(\omega) \cos\left(\omega t - \frac{\pi}{2} + \frac{1}{2} \arccos\left(\frac{A_{N2}}{r_N}\right) - \frac{|x|\sqrt{r_N}}{\sqrt{D}A_{N3}} \sin\left(\frac{1}{2} \arccos\left(\frac{A_{N2}}{r_N}\right)\right)\right) d\omega, \quad (\text{A.7})$$

where

$$\begin{aligned}
A_{N1} = & \sum_{j=0}^{(N-1)/2} (-1)^j K N_{N-2j} \omega^{1+2j} \\
& \times \left[ \sum_{l=0}^{(N-3)/2} (-1)^{1+l} (P N_{N-1-2l} - K N_{N-1-2l}) \omega^{2(1+l)} + \prod_{l=0}^N \lambda_l \right] \\
& - \sum_{j=0}^{(N-1)/2} (-1)^{1+j} K N_{N-1-2j} \omega^{2(1+j)} \\
& \times \left[ \sum_{l=0}^{(N-1)/2} (-1)^l (P N_{N-2l} - K N_{N-2l}) \omega^{1+2l} \right], \tag{A.8}
\end{aligned}$$

$$\begin{aligned}
A_{N2} = & \sum_{j=0}^{(N-1)/2} (-1)^{1+j} K N_{N-1-2j} \omega^{2(1+j)} \\
& \times \left[ \sum_{l=0}^{(N-3)/2} (-1)^{1+l} (P N_{N-1-2l} - K N_{N-1-2l}) \omega^{2(1+l)} + \prod_{l=0}^N \lambda_l \right] \\
& + \sum_{j=0}^{(N-1)/2} (-1)^j K N_{N-2j} \omega^{1+2j} \left[ \sum_{l=0}^{(N-1)/2} (-1)^l (P N_{N-2l} - K N_{N-2l}) \omega^{1+2l} \right], \tag{A.9}
\end{aligned}$$

$$\begin{aligned}
A_{N3} = & \left\{ \left[ \prod_{l=0}^N \lambda_l + \sum_{l=0}^{(N-3)/2} (-1)^{1+l} (P N_{N-1-2l} - K N_{N-1-2l}) \omega^{2(1+l)} \right]^2 \right. \\
& \left. + \left[ \sum_{l=0}^{(N-1)/2} (-1)^l (P N_{N-2l} - K N_{N-2l}) \omega^{1+2l} \right]^2 \right\}^{1/2}, \tag{A.10}
\end{aligned}$$

$$\Phi_N(\omega) = \frac{\sqrt{r_N}}{2\sqrt{D}A_{N3}\omega} \exp\left(-\frac{|x|\sqrt{r_N}}{\sqrt{D}A_{N3}} \cos\left(\frac{1}{2} \arccos\left(-\frac{A_{N2}}{r_N}\right)\right)\right) \tag{A.11}$$

and

$$r_N = \sqrt{A_{N1}^2 + A_{N2}^2}. \tag{A.12}$$

We note that  $KN_0 = 1$  for both cases.

## References

- [1] Kubo R, Toda M and Hashitsume N, 1985 *Statistical Physics II: Nonequilibrium Statistical Mechanics* (Berlin: Springer)
- [2] Bouchaud J P and Georges A, 1990 *Phys. Rep.* **195** 127
- [3] Risken H, 1996 *The Fokker-Planck Equation* (Berlin: Springer)
- [4] Wang K G and Tokuyama M, 1999 *Physica A* **265** 341

- [5] Metzler R and Klafter J, 2000 *Phys. Rep.* **339** 1
- [6] Zaslavsky G M, 2002 *Phys. Rep.* **371** 461
- [7] Balucani U, Lee M H and Tognetti V, 2003 *Phys. Rep.* **373** 409
- [8] Metzler R and Klafter J, 2004 *J. Phys. A: Math. Gen.* **37** R161
- [9] West B J, Geneston E L and Grigolini P, 2008 *Phys. Rep.* **468** 1
- [10] West B J and Picozzi S, 2002 *Phys. Rev. E* **65** 037106
- [11] Picozzi S and West B J, 2002 *Phys. Rev. E* **66** 046118
- [12] Golding I and Cox E C, 2006 *Phys. Rev. Lett.* **96** 098102
- [13] Kou S C and Xie X S, 2004 *Phys. Rev. Lett.* **93** 180603
- [14] Min W, Luo G, Cherayil B J, Kou S C and Xie X S, 2005 *Phys. Rev. Lett.* **94** 198302
- [15] Chaudhury S, Kou S C and Cherayil B J, 2007 *J. Phys. Chem. B* **111** 2377
- [16] Montroll E W and Weiss G H, 1965 *J. Math. Phys.* **6** 167
- [17] Scher H and Lax M, 1973 *Phys. Rev. B* **7** 4502
- [18] Shlesinger M F, 1974 *J. Stat. Phys.* **10** 421
- [19] Scher H and Montroll E, 1975 *Phys. Rev. B* **12** 2455
- [20] Klafter J and Silbey R, 1980 *Phys. Rev. Lett.* **44** 55
- [21] Kotulski M, 1995 *J. Stat. Phys.* **81** 777
- [22] Barkai E and Klafter J, 1997 *Phys. Rev. Lett.* **79** 2245
- [23] Coffey W T, Crothers D S F, Holland D and Titov S V, 2004 *J. Mol. Liq.* **114** 165
- [24] Balakrishnan V, 1985 *Physica A* **132** 569
- [25] Barkai E, Metzler R and Klafter J, 2000 *Phys. Rev. E* **61** 132
- [26] Fogedby H C, 1994 *Phys. Rev. Lett.* **73** 2517
- [27] Fogedby H C, 1994 *Phys. Rev. E* **50** 1657
- [28] Klafter J, Blumen A and Shlesinger M F, 1987 *Phys. Rev. A* **35** 3081
- [29] Berkowitz B, Cortis A, Dentz M and Scher H, 2006 *Rev. Geophys.* **44** RG2003
- [30] Baule A and Friedrich R, 2007 *Europhys. Lett.* **77** 10002
- [31] Wang K G and Lung C W, 1991 *Phys. Lett. A* **153** 423
- [32] Weissman H, Weiss G H and Havlin S, 1989 *J. Stat. Phys.* **57** 301
- [33] Havlin S and Weiss G H, 1990 *J. Stat. Phys.* **58** 1267
- [34] Barbi M, Place C, Popkov V and Salerno M, 2004 *Phys. Rev. E* **70** 041901
- [35] Barbi M, Place C, Popkov V and Salerno M, 2004 *J. Biol. Phys.* **30** 203
- [36] Saxton M J, 2007 *Biophys. J.* **92** 1178
- [37] Fa K S and Wang K G, 2010 *Phys. Rev. E* **81** 011126
- [38] Hilfer R and Anton L, 1995 *Phys. Rev. E* **51** R848
- [39] Balescu R, 1997 *Statistical Dynamics: Matter out of Equilibrium* (Singapore: Imperial College Press)
- [40] Fa K S, 2007 *Eur. Phys. J. E* **24** 139
- [41] Ryabov Y E, 2003 *Phys. Rev. E* **68** 030102(R)
- [42] Wlodarczyk J and Kierdaszuk B, 2003 *Biophys. J.* **85** 589
- [43] Carpinteri A and Mainardi F, 1997 *Fractals and Fractional Calculus in Continuum Mechanics* (Wien: Springer) pp 223–76
- [44] Erdelyi A, Magnus W, Oberhettinger F and Tricomi F G, 1955 *Higher Transcendental Functions* vol III (New York: McGraw-Hill)
- [45] Metzler R, Klafter J and Jortner J, 1999 *Proc. Nat. Acad. Sci.* **96** 11085
- [46] Vallejos R O, Mendes R S, da Silva L R and Tsallis C, 1998 *Phys. Rev. E* **58** 1346
- [47] Glockle W G and Nonnenmacher T F, 1995 *Biophys. J.* **68** 46
- [48] Montroll E W and Shlesinger M F, 1982 *Proc. Nat. Acad. Sci.* **79** 3380
- [49] Albuquerque E L and Cottam M G, 2004 *Polaritons in Periodic and Quasiperiodic Structures* (Amsterdam: Elsevier)